Weather and Climate Extremes 43 (2024) 100645

Contents lists available at ScienceDirect

Weather and Climate Extremes

journal homepage: www.elsevier.com/locate/wace

Hurricane track trends and environmental flow patterns under surface temperature changes and roughness length variations

Oussama Romdhani, Leo Matak, Mostafa Momen *

Department of Civil and Environmental Engineering, University of Houston, Houston, TX, USA

ARTICLE INFO

Keywords:
Hurricane simulation
Momentum roughness length
Surface friction
Ocean warming
Environmental flow
Tropical cyclone
Hurricane track

ABSTRACT

Given the significant damage that hurricanes can cause every year, accurate forecasts of these extreme weather events are crucial. Ocean warming can substantially impact the intensity and track of hurricanes in the future. Forecasting the track of hurricanes is typically more challenging than intensity predictions since tracks are influenced not only by hurricane vortex dynamics but also by global and synoptic weather systems (i.e., environmental flow). The dynamical mechanisms that modulate hurricane trajectories under changes in the surface temperature and friction are not comprehensively established yet. The primary objective of this paper is to address this knowledge gap by conducting six real hurricanes and some non-hurricane simulations using the Weather Research and Forecasting (WRF) model. In total, 90 WRF simulations are carried out to characterize the impacts of varying the surface temperature and drag on hurricane tracks and their relationship with environmental flow patterns. It is found that ocean warming tends to intensify hurricanes by ~20 % and decrease their azimuthal translational velocity, and vice versa when the surface is cooled. Hurricanes move more towards the west over the Atlantic Ocean when the surface temperature is decreased and vice versa. This was shown to be due to the changes in the average azimuthal speed of environmental flows. Increasing the surface temperature, destabilizes the atmosphere, and increases the surface friction velocity. Hence, increased surface friction appears to slow down the environmental flow and consequently hurricane track azimuthal translational speed. This finding was confirmed by another suite of simulations in which only the surface roughness length of the low-wind environmental flow regime was altered. It was shown that surface drag changes have a similar impact on hurricane tracks as surface temperature variations. Decreasing the default surface drag for low-wind regimes tends to further move the hurricanes toward the west and vice versa. This paper provides notable insights into future hurricane track trends and the role of ocean temperature and momentum exchange coefficients in hurricane track and environmental flow patterns. Moreover, the results of this study can be useful for advancing surface layer parameterizations and their impacts on hurricane track forecasts in weather/climate models.

1. Introduction

Hurricanes have been one of the most severe and expensive natural disasters in the US that have caused billions of dollars in damage since 1970 (Cheikh and Momen, 2020; Marsooli et al., 2019). Accurate prediction of hurricane tracks is typically challenging since global-scale and synoptic weather systems influence their trajectories in addition to their internal dynamics (Wang et al., 1998). Hurricane track predictions can become even more difficult with ocean warming (Emanuel, 2017), which is projected to modulate the synoptic weather systems (Studholme et al., 2022) and intensity of hurricanes (Emanuel, 2005; IPCC, 2023; Knutson et al., 2020, 2019; Mei and Xie, 2016; Walsh et al., 2019). Hence, given the unique dynamics of hurricane flows (Momen et al., 2021), it is essential to better understand and characterize the primary dynamical factors that influence hurricane tracks in order to enhance their forecasts.

A tropical cyclone (TC) vortex is embedded in and steered by a basic surrounding flow, aka environmental flow, which can theoretically be demarcated by removing the TC vortex from the environmental circulation field on the scale of a thousand kilometers. The environmental flow is a major factor that affects the TC's trajectory. This concept has been well established and applied by modelers in the track prediction of TCs (Kasahara, 1957; Miller and Moore, 1967; Roy and Kovordányi, 2012). The definition of the environmental flow usually modulates the empirical relationships between TC motion and surrounding large-scale

* Corresponding author.
E-mail address: mmomen@uh.edu (M. Momen).

https://doi.org/10.1016/j.wace.2024.100645
Received 17 April 2023; Received in revised form 7 January 2024; Accepted 19 January 2024
Available online 28 January 2024

Abbreviations

WRF	Weather Research and Forecasting
ARW	Advanced Research WRF
SST	Sea-Surface Temperature
TSK	Skin Temperature
TC	Tropical Cyclone
PBL	Planetary Boundary Layer

flows. Previous studies attempted to extract the environmental steering flow from observational circulation flow by spatially removing small-scale and large-scale disturbances using the Poisson equation for stream function and velocity potential (Galarneau and Davis, 2013). Prior studies hypothesized that the deep mean steering flow layer (between 1 000 and 100 hPa) typically approximates the actual TC motion (Dong and Neumann, 1983; Franklin, 1990; Velden and Leslie, 1991). These studies indicate that TC motion is mainly driven by the environmental flow field.

The environmental flow direction is strongly influenced by the sea-surface temperature (SST) and the surface layer characteristics. Ocean warming can influence the dynamics of these environmental flows and consequently the TC trajectories (Chu et al., 2023; Garner et al., 2021; Hall et al., 2021; Kossin et al., 2010). Some recent studies have shown that with global warming the translational speed of TCs has slowed down (Kossin, 2018). Several other studies predicted a poleward movement of TCs due to global warming (Fyfe et al., 1999; Kossin and Camargo, 2009; Kushner et al., 2001; Miller et al., 2006; Wu et al., 2011). This phenomenon can lead to a decrease in TC counts making landfall in the US, particularly over the southern Gulf of Mexico and the Caribbean (Colbert et al., 2013). These predictions were supported by the observations of a poleward shift in the southern hemisphere (Thompson and Solomon, 2002). The future TC tracks depend on the processes that modulate the temperature gradients (Shaw et al., 2016). Some numerical studies using idealized models showed a poleward shift in the westerlies or jet streams in response to increases in SST gradients (Son and Lee, 2005), stratospheric temperature gradients (Haigh et al., 2005; Polvani and Kushner, 2002), and eddy length scales (Kidston et al., 2011). Chen et al. (2007) studied the dynamical mechanisms underlying the poleward shift by simply modifying the magnitude of the surface friction, which according to Robinson (1997) drives the westerlies and the midlatitude jet poleward in response to altered surface drag. Hence, it is vital to understand whether such changes on the surface drag of environmental flows have any impacts on TC dynamics and track.

Numerical weather prediction (NWP) models enable us to quantify the impacts of surface temperature and drag on hurricane tracks. The Weather Research and Forecasting (WRF) model is the state-of-the-art NWP system that has been widely used in TC forecasts (Abarca and Corbosiero, 2011; Chen et al., 2011; Davis et al., 2008; Nasrollahi et al., 2012; Powers et al., 2017). Despite the recent progress in improving turbulence models (Li et al., 2023; Romdhani et al., 2022) and planetary boundary layer (PBL) parameterizations (Jiménez et al., 2012; Matak and Momen, 2023; Nolan et al., 2009; Vaughan and Fovell, 2021; Zhang et al., 2011) for hurricane flows, there has not been a thorough NWP study that extensively determines the effects of ocean temperature and surface friction variations on TC tracks.

The objective of this paper is to address this knowledge gap by characterizing the impacts of surface temperature and drag on some recent hurricane tracks and environmental flow patterns. This is particularly important given that the mesoscale and microscale dynamical factors that impact hurricane tracks have received less attention compared to hurricane intensity studies (e.g., Balaguru et al., 2018; Gopalakrishnan et al., 2013; Zhang et al., 2015). This goal will be achieved by conducting a comprehensive set of WRF simulations where the surface temperature and drag are altered for hurricane and non-hurricane scenarios. In particular, the research questions of the present paper are:

1) What are the impacts of changing ocean temperature on hurricane track and dynamics?
2) How do surface temperature variations influence the environmental flow patterns, and do these affect hurricane tracks?
3) How does ocean warming modulate the surface friction, and does altering the surface drag have a similar effect on hurricane tracks and environmental flow patterns?

The current paper addresses these questions as follows. Section 2 describes the selected hurricanes, the numerical framework, and the details of the surface layer scheme. Then, the section provides an overview of the conducted WRF simulations. Section 3 presents the simulation results of hurricane track and intensity under surface temperature changes (question 1). The next part of the section analyzes the response of the environmental flow and surface friction to altered surface temperatures (question 2). Then, the response of the environmental flow to surface drag parametrizations and its impacts on hurricane tracks are discussed (question 3). Finally, Section 4 summarizes the key findings of the paper.

2. Methods

2.1. Simulation cases and numerical domains

To characterize the impacts of the surface temperature and drag on simulated TC tracks, historical hurricanes were chosen. These hurricanes were chosen based on their trajectory such that they become category 4 or 5 (major TCs) as they move into the Atlantic basin. Another criterion for the case selection was focusing on newer hurricanes after 2010 to include more recent data. Fig. 1 shows the track of the chosen hurricanes and their simulation domain. In total, six TCs of categories 4 or 5 between 2010 and 2020 were selected.

The first chosen hurricane, which occurred in 2020, is Teddy. It originated from a strong tropical wave near the African west coast and continued moving west and northwest around a strong subtropical ridge in the central Atlantic (Blake, 2020). Similarly, Lorenzo moved initially westward to northwestward steered by a subtropical ridge to its north. By September 29th, 2019, Lorenzo became a category 5 hurricane when its peak intensity reached 72 m s^{-1} (Zelinsky, 2019). Earl, initially a tropical wave, departed the West African coast on August 23rd before acquiring sufficient convective organization to be considered a TC by August 25th. Earl strengthened gradually as it was steered northwestward and then rapidly weakened as it turned northward (Cangialosi, 2011). Florence, originated from a convectively tropical wave, and made landfall near North Carolina on September 14, 2018 (Stewart and Berg, 2019). The two other selected hurricanes are Maria (Hosannah et al., 2021; Pasch et al., 2023) and Gonzalo (Brown, 2015). More details about these hurricanes and their simulations period are provided in Table 1.

To determine the impacts of ocean warming and surface drag on the environmental flow patterns, we also conducted a suite of simulations for 12 weeks during the Atlantic hurricane season spread over two years. The objectives of running these non-hurricane cases were 1) to comprehensively assess the patterns developed in the direction of the environmental flow in the absence of hurricane vortex interactions, 2) to determine whether changes in hurricane track are caused by the global environmental flow patterns, and 3) to have a broader characterization of the synoptic weather system across a larger range of latitudes. Hence, we ran 7-day simulations for each month of the hurricane season (June–November) for two years in a larger domain. The details about the domain size and the timeframe of these simulations are provided in

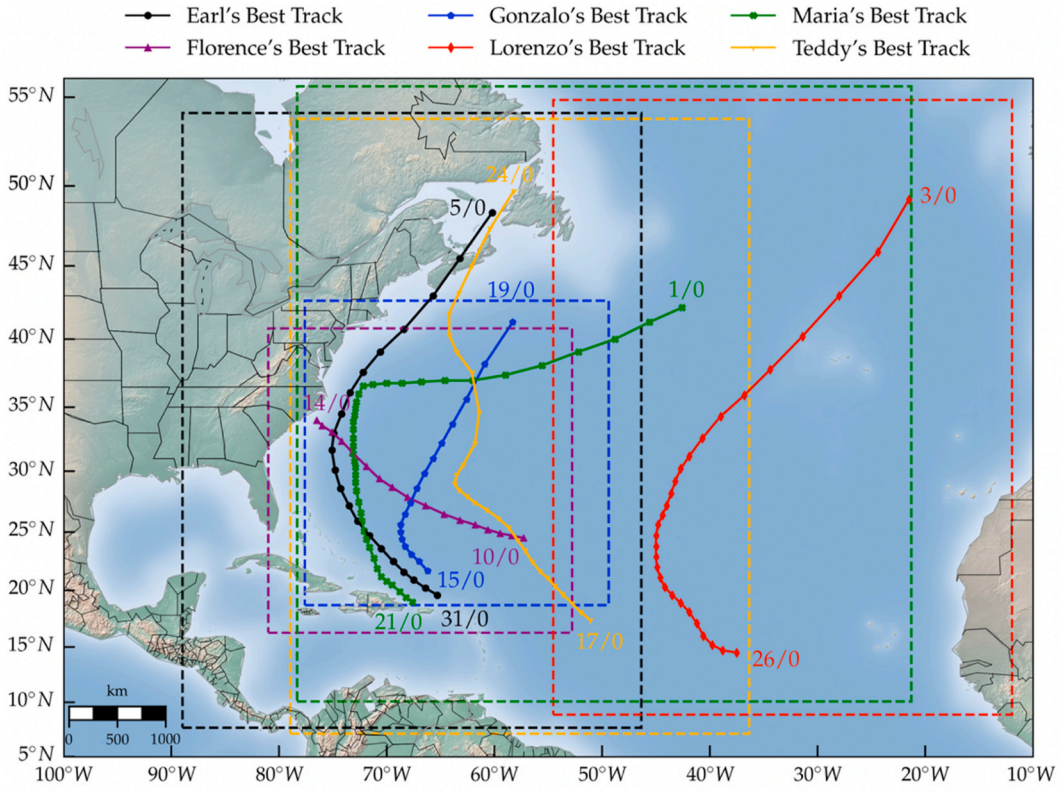

Fig. 1. Best-observed track of the six chosen hurricanes for this study. The solid lines represent the hurricane trajectory during the simulation timeframe, and the dashed boxes display the size of the simulated domain for each hurricane. The markers indicate the hurricane's eye, labeled with timestamps in day/hour format. These timestamps correspond to the start and end times of the simulation for each case.

Table 1
List of investigated hurricanes and their simulation periods in WRF.

Hurricanes	Year	Category	Formation to Dissipation Dates	Simulation Running Hours	Approximate Domain Size	Observed Max Speed
Teddy	2020	4	Sept. 12 – Sept. 24	168 h, Sept. 17, 12 a.m. – Sept. 24, 12 a.m.	4 800 km × 6 400 km	62 m s^{-1}
Maria	2017	5	Sept. 16 – Oct. 2	264 h, Sept. 21, 12 a.m. – Oct. 1, 12 a.m.	6 400 km × 6 400 km	77 m s^{-1}
Lorenzo	2019	5	Sept. 23 – Oct. 4	168 h, Sept. 26, 12 a.m. – Oct. 3, 12 a.m.	4 800 km × 6 400 km	72 m s^{-1}
Florence	2018	4	Aug. 31 – Sept. 18	96 h, Sept. 10, 12 a.m. – Sept. 14, 12 a.m.	3 200 km × 3 200 km	67 m s^{-1}
Gonzalo	2014	4	Oct. 12 – Oct. 20	96 h, Oct. 15, 12 a.m. – Oct. 19, 12 a.m.	3 200 km × 3 200 km	64 m s^{-1}
Earl	2010	4	Aug. 25 – Sept. 6	120 h, Aug. 31, 12 a.m. – Sept. 5, 12 a.m.	4 800 km × 6 400 km	64 m s^{-1}

Table 2
List of simulated timeframes and their corresponding domain size for non-hurricane cases. For all cases, the domain size is approximately 8 000 km × 8 000 km.

Month	Years	Simulation Running Hours
June	2019, 2020	168 h, Jun. 1, 12 a.m. – Jun. 8, 12 a.m.
July		168 h, Jul. 1, 12 a.m. – Jul. 8, 12 a.m.
August		168 h, Aug. 1, 12 a.m. – Aug. 8, 12 a.m.
September		168 h, Sept. 1, 12 a.m. – Sept. 8, 12 a.m.
October		168 h, Oct. 1, 12 a.m. – Oct. 8, 12 a.m.
November		168 h, Nov. 1, 12 a.m. – Nov. 8, 12 a.m.

Table 2.

2.2. Numerical Methodology

In this study, we employ the Advanced Research WRF (ARW) model version 4.1.3 to conduct the simulations. This code is developed and maintained by the National Center for Atmospheric Research (NCAR), and solves fully compressible, non-hydrostatic Euler equations (Skamarock et al., 2019). In addition to different meteorological applications such as urban meteorology (e.g., Li et al., 2014; Olivo et al., 2017), hydrometeorology (e.g., Yang et al., 2015), and air quality (e.g., Cuchiara et al., 2014) the code has been extensively employed in hurricane simulation studies (Cavallo et al., 2013; Davis et al., 2008; Fierro et al., 2009; Romdhani et al., 2022). The ARW package contains multiple options for the physics suite. The vertical diffusion in this code is handled by the PBL scheme. In this paper, the non-local Yonsei University [YSU (Hong, 2010; Hong et al., 2006);] scheme is employed, which is the recommended model for TC simulations by the ARW guideline (Skamarock et al., 2019).

2.2.1. Changing the surface temperature

To characterize the impacts of ocean temperature on the TC track, we conducted a suite of simulations by varying the default surface temperature [i.e., the output variable surface skin temperature (TSK)] by 2 K. The selected value is consistent with the increase in ocean warming that is projected to be ~1.3-2.4° K by year 2100 under moderate emissions scenario of the sixth assessment report of the Intergovernmental Panel on Climate Change (IPCC, 2023; IPCC, 2013; Meinshausen et al., 2020, 2011; Rogelj et al., 2018; Schleussner et al., 2016). Altering the surface temperature will impact both the environmental flow and hurricane vortex dynamics which will be discussed in Section 3. An

example of Hurricane Florence runs is shown in Fig. 2, in which the surface temperature is decreased (top panels) and increased (bottom panels) compared to the default case (middle panels). The figure shows how the surface temperature change is implemented in WRF (left panels) and how this change affects the surface wind speed of the simulated TCs (right panels). A similar result for Hurricane Teddy is provided in supplementary Fig. A1. These impacts will be characterized in the results section.

2.2.2. Changing the momentum roughness length

The ARW model employs three formulations to model the surface fluxes: One formulation for regular weather prediction based on the PBL scheme (Skamarock et al., 2019), and two formulations specifically designed for TCs. The first TC-specific formulation implements Donelan et al. (2004) formula for the momentum exchange coefficient C_D and a constant thermal and moisture roughness length ($z_{0q} = 10^{-4}$ m) for temperature and moisture exchange coefficient C_K. We refer to this parametrization as *Isftcflx* = 1 following the ARW's notation. The second TC-specific formulation is a modification of the Donelan parameterization using Garratt's formulation (Garratt, 1994), which hereafter is referred to as *Isftcflx* = 2. In the current study, both parametrizations are used for TC simulations. The performance of these two parameterizations has been previously tested by NCAR's real-time hurricane runs in 2012 (NCAR, 2019).

The surface momentum flux in ARW is defined as

$$\tau = -\rho C_D U_L^2. \tag{1}$$

In equation (1), τ refers to the surface momentum and represents momentum exchange between the ocean and the overlaying atmosphere, ρ is the air density, and U_L is the wind speed at the model's lowest level (Ming et al., 2023). Finally, C_D is a dimensionless exchange coefficient for the momentum (drag coefficient), which is defined as

$$C_D = \left(\frac{\kappa}{ln(z/z_0) - \psi_m(z/L)}\right)^2, \tag{2}$$

where κ is the von Kármán constant (=0.4), z is the height above the surface, z_0 is the momentum roughness length (Momen and Bou-Zeid, 2016) and ψ_m is an atmospheric stability correction term that is a function of z and Obukhov length L (Momen, 2022). The stability function ψ_m is positive for unstable conditions and negative for stable conditions.

Determining the exact drag coefficient for strong TC winds is an active research area (Jarosz et al., 2007; Li et al., 2023; Powell et al., 2003; Soloviev et al., 2014), in which some studies indicate that C_D reaches its maximum of 0.003 for TCs with wind speeds ~35 m s^{-1} and then levels off as the wind speed further increases (Black et al., 2007;

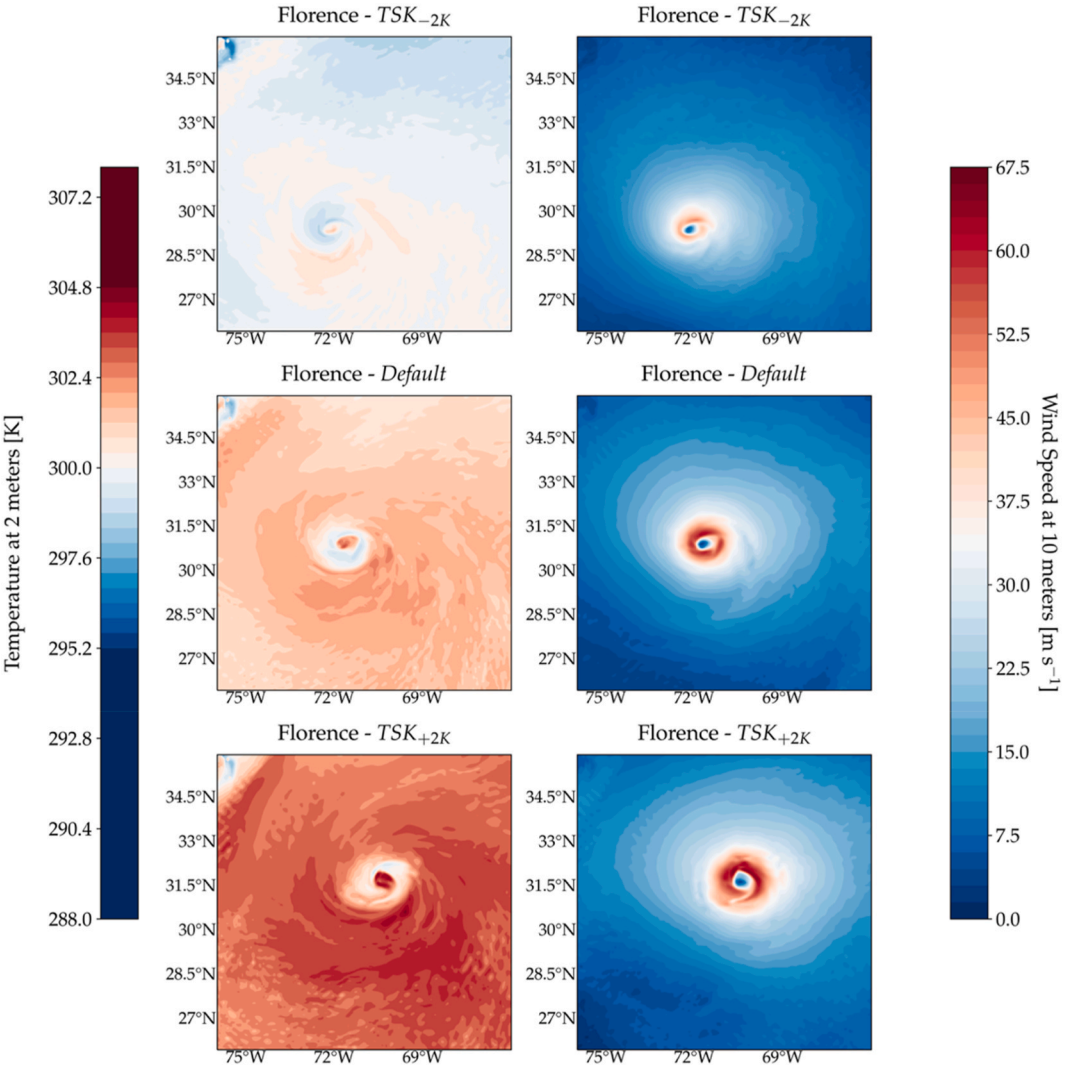

Fig. 2. Contour maps depicting the temperature at 2 m and the wind speed at 10 m for Hurricane Florence after 60 h of simulation. The left column shows temperature contour maps for (top) TSK_{-2K}, (middle) default, and (bottom) TSK_{+2K} cases, and the right column depicts the corresponding surface wind speed contours.

Davis et al., 2008). Hence, Donelan's momentum roughness length in the ARW code is calculated as

$$z_0 = \max\left[1.27\times10^{-7}, \min\left[z_w z_2 + (1-z_w)z_1, 2.87\times10^{-3}\right]\right], \tag{3.a}$$

$$z_w = min\left(1, \left[\frac{u_*}{1.06}\right]^{0.3}\right), \tag{3.b}$$

$$z_1 = 0.011\frac{u_*^2}{g} + 1.59\times10^{-5}, \tag{3.c}$$

$$z_2 = \frac{10}{\exp\left(9.5u_*^{-\frac{1}{3}}\right)} + \frac{1.65\times10^{-6}}{\max(u_*, 0.01)}, \tag{3.d}$$

where u_* represents the friction velocity defined as

$$u_* = \frac{\kappa U}{\ln\left(\frac{z}{z_0}\right) - \psi_m(z/L)}. \tag{4}$$

Equation (4) shows that by increasing z_0, we effectively increase u_* and vice versa. Similar impacts can be seen for changing the stability correction function for which destabilizing surface heat fluxes ($\psi_m > 0$) increase u_* and vice versa.

In this study, we change the default z_0 parameterization in WRF. This is to determine if changing the surface friction has similar impacts as varying the surface temperature on TC tracks and environmental flow patterns. Since the focus of this study is on understanding the role of environmental flows in modulating TC tracks, this change in the z_0 will only be applied to low-wind environmental flow regions. To separate the environmental flow from the TC vortex, we implemented the following formula

$$z_0 = \begin{cases} C_{Lz} \times z_0 \text{ if } V < V_{min} \\ (A \times (V - V_{max}) + 1) \times z_0 \text{ if } V_{min} < V < V_{max} \\ z_0 \text{ if } V > V_{max} \end{cases}, \tag{5}$$

where C_{Lz} refers to a newly defined coefficient that controls the magnitude of z_0, V denotes the surface wind speed at 10 m, $V_{\min}$ and $V_{\max}$ are the surface wind speed range over which we linearly change the roughness length, and $A \equiv (1 - C_{Lz})/(V_{max} - V_{min})$. For all the cases in this paper, they were chosen to be $V_{\min} = 20$ m s^{-1} and $V_{\max} = 30$ m s^{-1}. Hence, the changes in the roughness length will not be applied for hurricane vortex winds greater than 30 m s^{-1}.

Fig. 3 depicts an example of the implemented z_0 parametrization as a function of the surface wind speed. Depending on the implemented coefficient C_{Lz}, the z_0 is either increased ($C_{Lz} = 100$, top panels) or

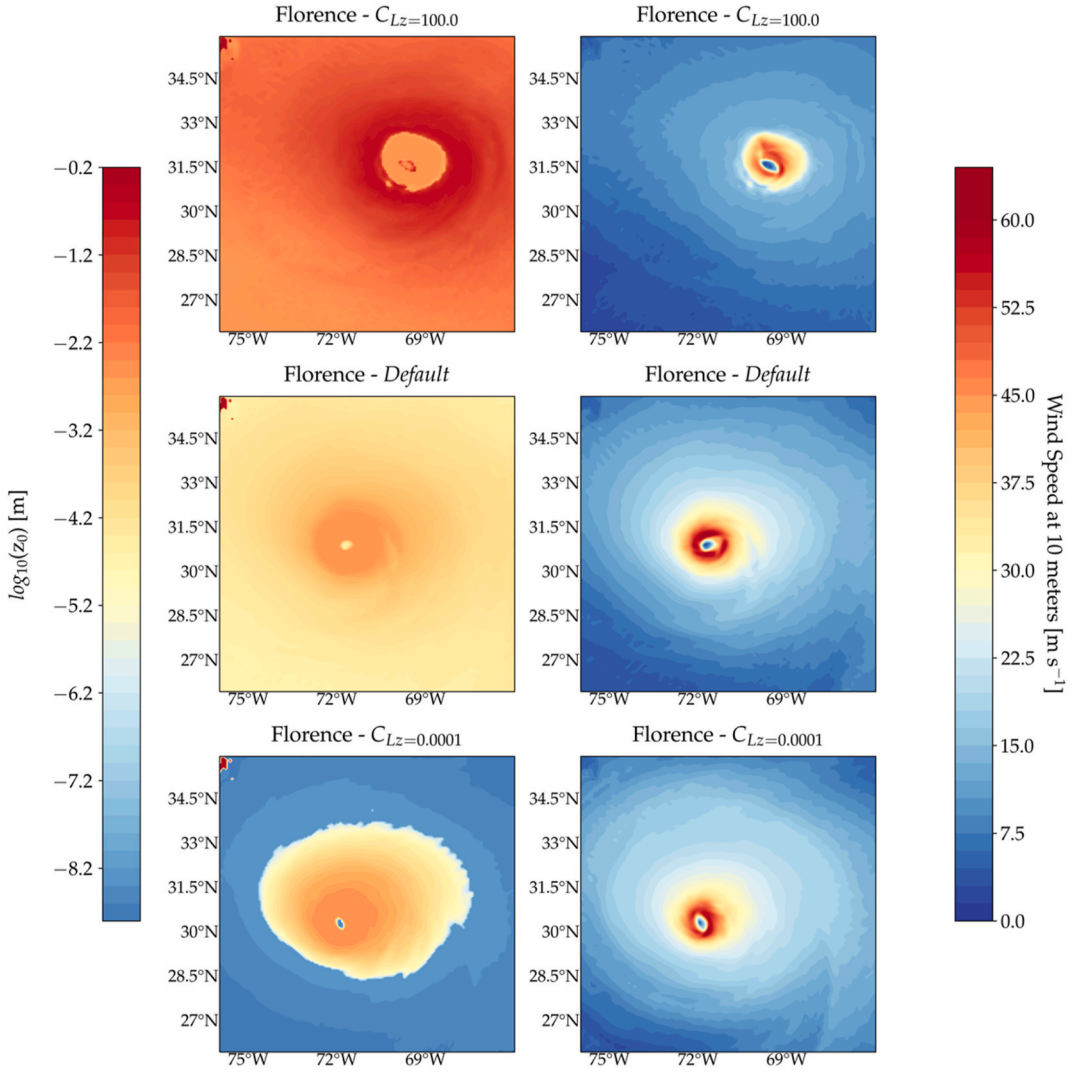

Fig. 3. Contour maps depicting the roughness length and the surface wind speed for Hurricane Florence after 60 h of simulation for *Isftcflx* = 1. The left column shows roughness length contours with C_{Lz} = (top) 100, (middle) 1, and (bottom) 0.0001, and the right column depicts their corresponding wind speed contours.

decreased ($C_{Lz} = 0.0001$, bottom panels) in the regions away from the TC eyewall compared to the default case ($C_{Lz} = 1$, middle panels). Regions where the surface wind speed surpasses V_{max} remained unchanged and in regions with wind speed lower than V_{min} the z_0 changes were in full effect. For instance, the low-wind environmental flow regions (blue colors in right panels of Fig. 3) experience a full z_0 change. In the case of $C_{Lz} = 100$ (Fig. 3, top panels), the z_0 of these regions increased (more red colors in the top left panel) compared to the default case (middle left panel). Similarly, in the case of $C_{Lz} = 0.0001$, the z_0 of these regions decreased (more blue colors in the bottom left panel) compared to the default case (middle left panel). A similar result was obtained for other hurricanes such as Hurricane Teddy (please see supplementary Fig. A.2). The impacts of these changes on TC tracks and environmental flow patterns will be discussed in Section 3.3.

2.3. Suites of WRF simulations

Two sets of ARW simulations are conducted in this study to examine how changes in surface temperature and drag affect TC tracks. First, we assess the impacts of altering the surface temperature on hurricane tracks and environmental flow patterns. To this end, six hurricanes of category 4 or 5 (see Table 1) are simulated by increasing and decreasing the default surface temperature by 2 K. Furthermore, to determine the role of environmental flow patterns in TC tracks 12 non-hurricane cases of Table 2 are also simulated under similar surface temperature changes. A summary of the conducted WRF simulations along with their naming convention is listed in Table 3. These simulations were carried out using an 8 km grid resolution for six real hurricanes and a 32 km grid resolution for 12 non-hurricane cases (due to their larger domain size), resulting in 6×3 (hurricane) $+12 \times 3$ (non-hurricane) $= 54$ ARW simulations. In the second set of simulations, the impacts of altering surface drag on TC tracks and environmental flow patterns and their analogies with surface temperature are characterized. A similar set of cases is carried out in this suite by keeping the default surface temperature but varying the default momentum roughness lengths (bottom rows of Table 3). These result in 36 new ARW cases, leading to a total of 90 simulations. Hereafter, we refer to the simulations in which no new changes in the surface temperature (TSK+0 K) and friction ($C_{Lz} = 1$) are applied as the default cases (control runs). In these simulations, the default WRF configurations are used to conduct historical hurricane simulations.

3. Results and discussion

3.1. Impacts of surface temperature changes on hurricane track and intensity

In this section, the results of the first set of hurricane simulations, in which the surface temperature of TC cases is varied, are presented (6 hurricanes under three surface temperatures). First, the impacts of surface temperature changes on atmospheric stability are examined. Fig. 4 shows the vertical profiles of potential temperature for the three imposed surface temperature scenarios. These profiles are averaged over a radius (R) band with respect to the radius of maximum wind (R_{MW}, as shown in supplementary Fig. B1). This non-dimensional radius band average ensures that the results represent the same dynamics in the parameter space of different hurricanes, which can have various sizes.

In general, the potential temperature profiles for the default cases (green lines) indicate neutral atmospheric stability in the hurricane boundary layer (HBL), which extends to ~500 m on average. This is consistent with the fact that shear production in hurricanes is the primary factor contributing to the turbulent kinetic energy and is much larger than the buoyancy production term in the outer eyewall region (Kepert, 2012; Sabet et al., 2022; Zhang et al., 2009). Hence, since the wind shear in HBLs is remarkably high, the ratio of buoyancy to shear production (i.e., the magnitude of the flux Richardson number) decreases and the HBL in the outer eyewall region tends to be in neutral stability (Yu et al., 2008; Zhang et al., 2009). When we increase the surface temperature by 2 K, the height where the inversion layer starts increases (red lines) and when we decrease the surface temperature the inversion layer elevation decreases (blue lines). In both scenarios, the atmosphere maintains its neutral stability. This inversion layer and its associated Richardson number have been a criterion for determining the PBL height (referred to as the thermodynamic BL height) in some PBL parameterizations such as the YSU scheme. The PBL height determines the vertical mixing and diffusion in hurricanes and highly affects the near surface wind speed (Momen et al., 2018, 2021; Momen and Bou-Zeid, 2017). Similar results were found for non-hurricane cases with the exception that the atmosphere in those cases is not necessarily neutral as in hurricane cases (please refer to supplementary Fig. C1 for more details).

These changes in surface temperature significantly impact the intensity of hurricanes. Fig. 5 displays the hurricane wind intensity timeseries versus the best observed near-surface maximum wind speed data from the US National Hurricane Center (Blake, 2020; Brown, 2015; Cangialosi, 2011; Pasch et al., 2023; Stewart and Berg, 2019; Zelinsky, 2019). In general, the results indicate that an increase of the surface temperature (red lines) generates stronger winds near the surface. For instance, Hurricane Gonzalo reached an intensity of ~47 m s^{-1} after 66 h of simulation for the default case (green line). When the surface temperature was increased by 2 K, the intensity increased to ~71 m s^{-1} (red line). Similarly, a decrease in the surface temperature reduces the near surface wind intensity (blue lines in Fig. 5). This finding is consistent with the hurricane's maximum potential intensity (MPI) theory (Emanuel, 1997) that predicts that TC's maximum wind speed is a function of the surface temperature minus the outflow temperature, and as this difference increases the TC can be more intense. Warmer ocean water increases the atmospheric heat uptake and provides an extra energy source for the TC. Hence, by increasing the surface temperature the energy content of the hurricane system rises and it can generate stronger winds.

To quantify the impacts of the surface temperature on hurricane intensity, the average near surface wind intensity over all hurricane cases is calculated. Fig. 6 shows the average wind intensity of the 6 hurricanes listed in Table 1, and the black bar depicts the average of the best observed data. As Fig. 6 indicates, the average wind intensity increases by ~20.6 % when the surface temperature is increased by 2 K. This result is consistent with recent evidence that TCs are becoming stronger with global warming (Emanuel, 2020; IPCC, 2023; Knutson et al., 2020, 2010; Walsh et al., 2019). On the other hand, the default wind intensity in the considered TCs reduces by ~19.6 % when the surface temperature is decreased by 2 K. Hence, the results indicate that a 2 K ocean warming can further increase the wind intensity of the considered category 4–5 hurricanes by ~20 %, making them an even stronger TC.

Table 3
The suites of ARW simulations conducted for the analysis of the impacts of *TSK* and z_0 on hurricane track and environmental flow patterns. Each hurricane case is named according to the following format *X*_Rkm_*V* where *X* is a placeholder for the hurricane name ("Ea" for Earl, "Fl" for Florence, "Go" for Gonzalo, "Lo" for Lorenzo, "Ma" for Maria, and "Te" for Teddy), *R* is the resolution, and *V* is the varied variable (*TSK* for the first set of simulations or C_{Lz} for the second suite). Non-hurricane cases are named as *M_Y*_Rkm _*V* in which *M* denotes the month and *Y* the year of the simulation according to Table 2.

Surface Variable	Value of change	Hurricane cases	Non-Hurricane cases
TSK	−2 K	*X*_8 km _TSK_{-2K}	*M_Y*_32 km_TSK_{-2K}
	0	*X*_8 km _TSK_{0K}	*M_Y*_32 km_TSK_{0K}
	+2 K	*X*_8 km _TSK_{+2K}	*M_Y*_32 km_TSK_{+2K}
C_{Lz}	0.0001	*X*_8 km_C_{Lz}=0.0001	*M_Y*_32 km_C_{Lz}=0.0001
	1	*X*_8 km_C_{Lz}=1	*M_Y*_32 km_C_{Lz}=1
	100	*X*_8 km_C_{Lz}=100	*M_Y*_32 km_C_{Lz}=100

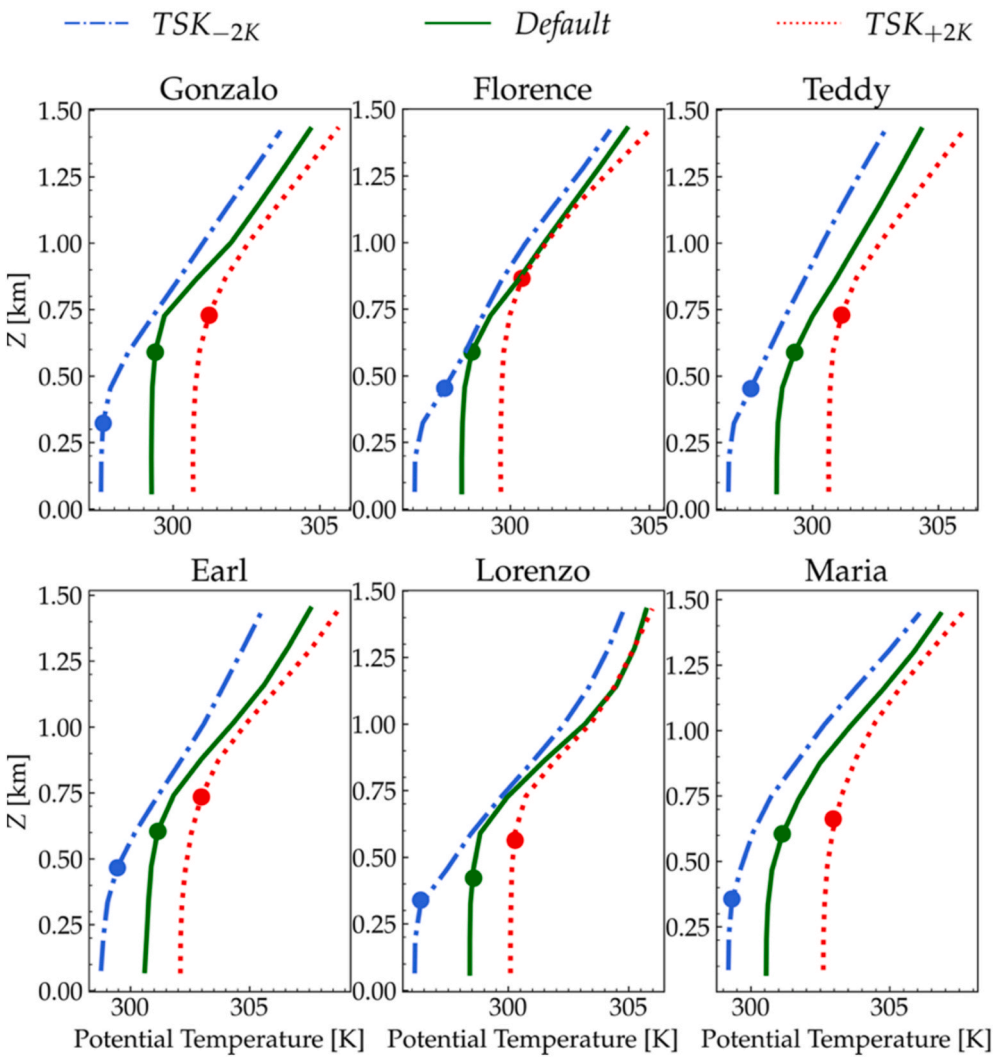

Fig. 4. Average potential temperature vertical profiles for all simulated hurricanes in terms of ocean temperature changes. The profiles are averaged over a range of R/R_{MW} between 1.6 and 1.7 where R is the radius from the hurricane center and R_{MW} is the radius of the maximum wind speed. The markers correspond to the PBL height output of WRF spatially averaged over the same region.

Altering the surface temperature also significantly impacts hurricane tracks. Fig. 7 shows the track for the six simulated hurricanes under different surface temperatures. At lower latitudes (below ~30°N), the TCs tend to propagate more toward the west as the surface temperature decreases (blue lines in Fig. 7). In contrast, when the default surface temperature increases, the results indicate that TCs move with a lower speed to the west (red lines in Fig. 7) compared to the default cases. This trend appears to be consistent in most considered hurricanes demonstrating that surface temperature can considerably modulate the TCs track.

To quantify the response of the simulated TC tracks to changing the surface temperature, we calculated the average longitudinal translational velocity of all considered hurricanes as a function of the surface temperature variations. Fig. 8 depicts the mean longitudinal traveling velocity of the hurricane vortex before and after its track recurves from moving west to east. This track recurvature separation allows us to distinguish the sign of TC motions. Fig. 8 shows that by decreasing the default surface temperature the longitudinal velocity increases by ~0.3 m s^{-1} toward the west before recurvature (left panel in Fig. 8). However, when we increase the surface temperature (red bars), the longitudinal velocity toward the west is decreased. After the recurvature (latitude $\gtrsim$ 35°), the trend for the magnitude of the translational velocity remains the same but its sign is reversed. The longitudinal velocity is increased for colder surface temperature (blue bars in the right panel of Fig. 8) toward the east, and it is decreased for warmer surface temperatures.

3.2. Analysis of the impacts of surface temperature changes on environmental flow patterns

In this section, the impacts of changing the surface temperature on environmental flow patterns and its relationship with TC tracks are discussed. To this end, the results of the conducted set of non-hurricane simulations as defined by Table 2 are presented. First, the impacts of surface temperature changes on the azimuthal velocity of the environmental flow are described.

After conducting all 12 non-hurricane cases for each surface temperature, the azimuthal wind velocity components are averaged at each latitude in the entire simulation domain which includes the Atlantic Ocean basin. The average azimuthal wind velocity is shown in Fig. 9 as a function of latitude for three surface temperature scenarios. The figure shows that increasing the surface temperature by 2 K (red line) tends to decrease the average azimuthal wind velocity towards the west below ~35° of latitude and then decrease it towards the east above ~35° compared to the default case (green line). A reverse trend can be observed when decreasing the surface temperature (blue line in Fig. 9) compared to the default case. This observed trend in the environmental

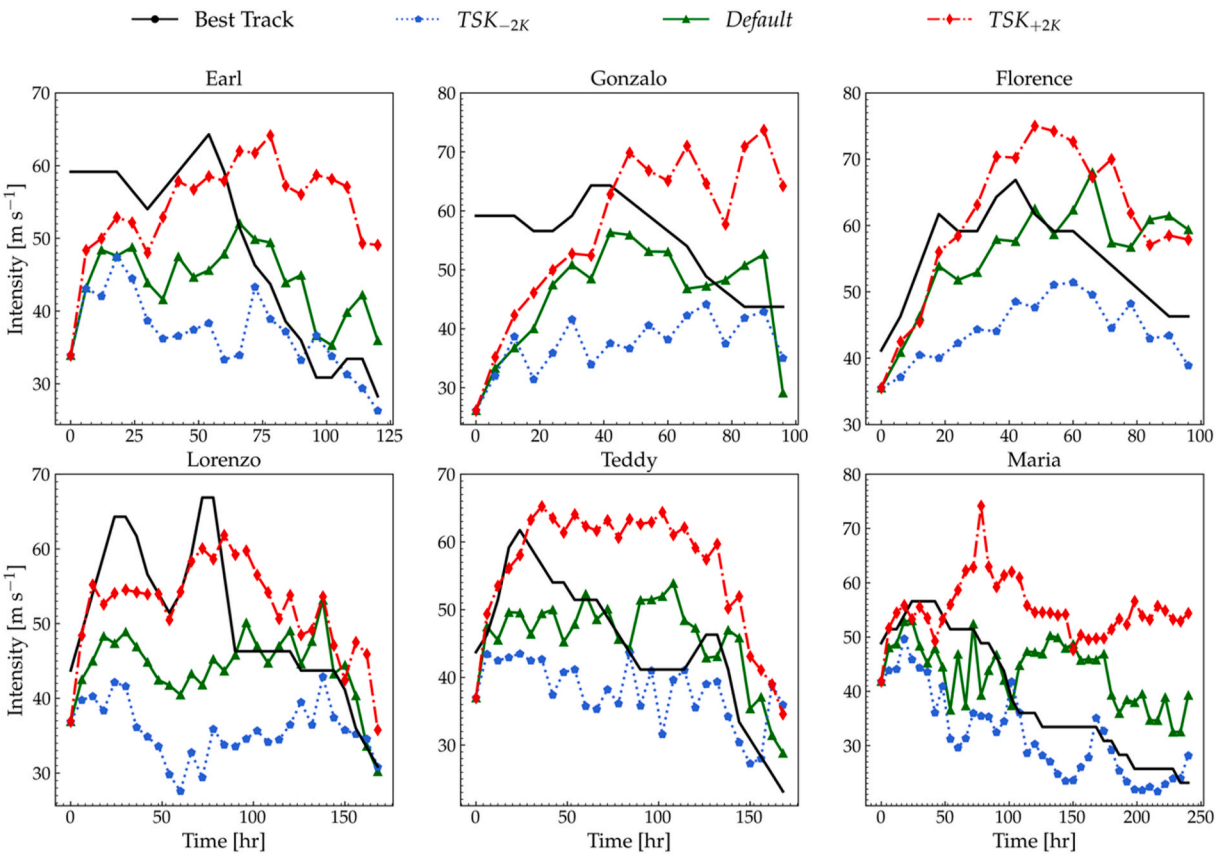

Fig. 5. Near-surface wind intensity timeseries in terms of changing the surface temperature for all considered hurricane cases. The black line depicts the best observed data.

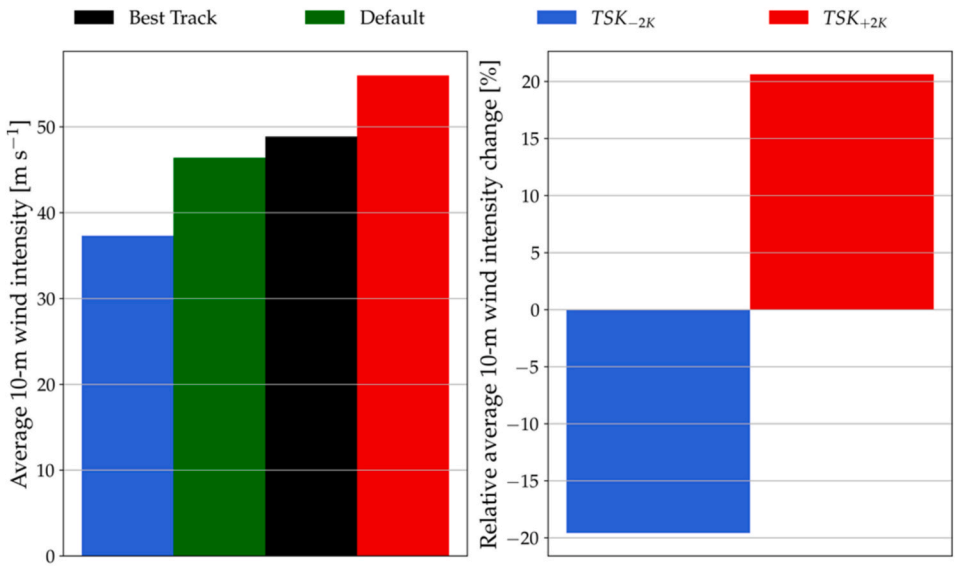

Fig. 6. (Left) Average wind intensity for all six simulated hurricanes in terms of surface temperature variations. The black bar depicts the average wind intensity of the hurricanes from the best-track observed data. (Right) the relative hurricane wind intensity changes in comparison to the default cases.

flow pattern is consistent with hurricane motions in Fig. 8 and can explain why such changes in TC tracks are observed as the surface temperature is altered. Further analysis and discussion of this change in the environmental flow patterns come as follows.

To assess the reason for this change in the environmental flow pattern, we investigated the PBL dynamics in the considered cases. To this end, the impacts of the surface temperature changes on eddy diffusivity profiles are described. Fig. 10 depicts the vertical profiles of the momentum exchange coefficient K_m. These profiles are obtained by averaging the largest 100 profiles over the ocean (sorted based on the maximum value of each profile). As Fig. 10(a) indicates, increasing the surface temperature (red line) increases the eddy diffusivity and vice versa.

In the YSU PBL scheme, the momentum exchange coefficient K_m is

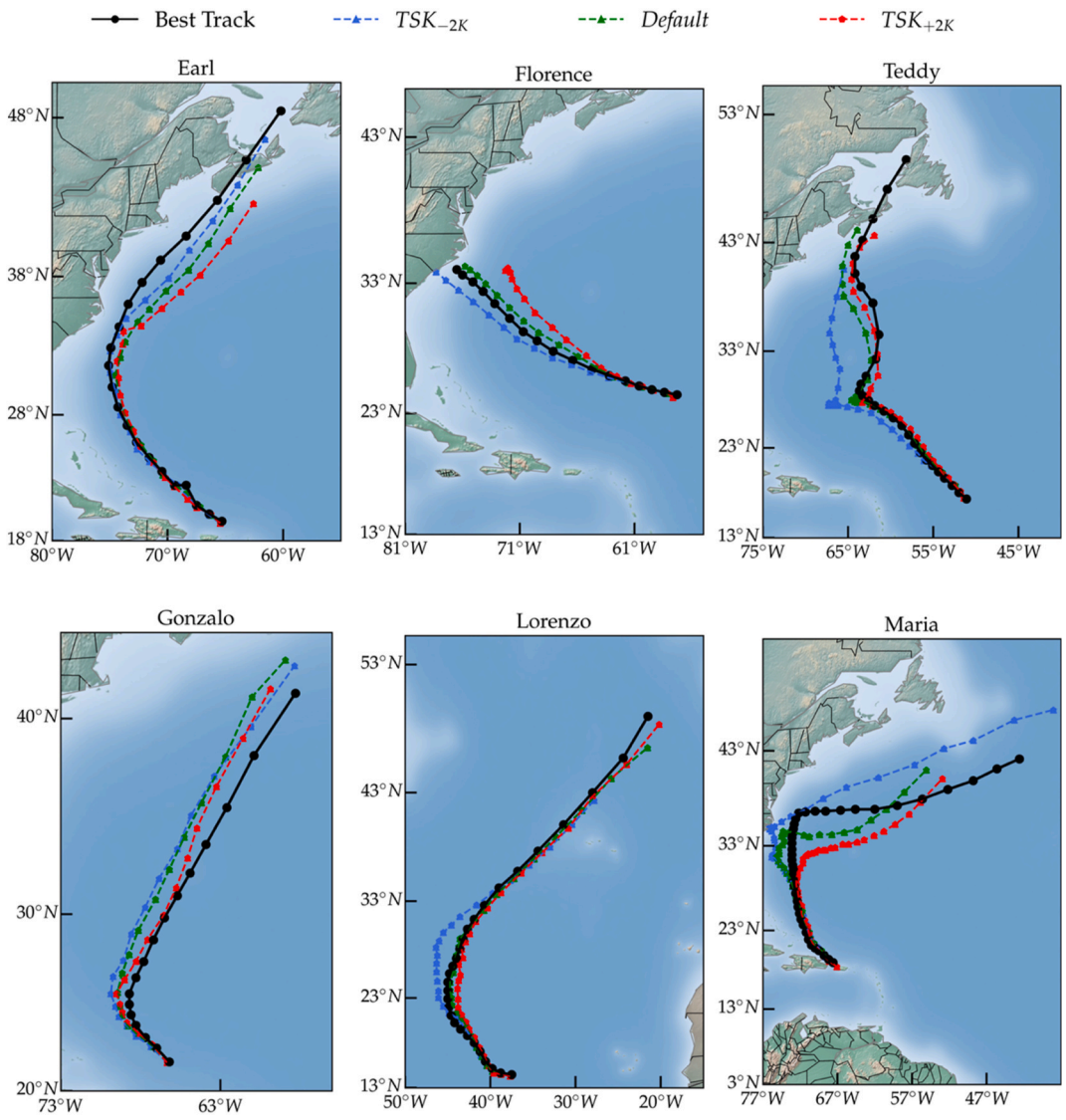

Fig. 7. The simulated track results of the three surface temperature scenarios in all considered hurricanes for an 8 km grid size.

calculated as

$$K_m(z) = \frac{\kappa u_*}{\varphi_m} z\left(1 - \frac{z}{h}\right)^p, \tag{6}$$

where κ is the von Kármán constant, z is the height above the surface, h is the PBL height, p is an exponent for the profile shape (in YSU, $p = 2$), and φ_m is the atmospheric stability correction. The increase in K_m in Fig. 10 (a) is mainly due to the change in u_*/φ_m. In fact, according to $u_* = \kappa U/[\ln(z) - \ln(z_0) - \psi_m(z/L)]$, we expect that by increasing the surface temperature and destabilizing the PBL ($\psi_m(z/L) > 0$), u_* also increases. We verified this increase in u_* in the increased surface temperature cases by calculating the average friction velocity in the conducted simulations (see supplementary Fig. D1). Hence, it appears that increasing the surface temperature increases mixing in the PBL and leads to higher surface friction and vertical diffusion. This higher diffusion reduces the azimuthal velocity in the environmental flows as shown in Fig. 9.

To corroborate this finding that friction and mixing variation is the cause of changes in the environmental flow patterns, a similar set of simulations were conducted in which only the surface drag is altered. As Fig. 10(b) shows, higher roughness length z_0 (red line in Fig. 10(b)) also yields a higher eddy diffusivity compared to the default run (green line in Fig. 10(b)) and vice versa. This is again expected because higher imposed z_0 increases the friction velocity in a similar manner to increasing the surface heat flux (see $u_* = \kappa U/[\ln(z) - \ln(z_0) - \psi_m(z/L)]$, and supplementary Fig. D1, right panel). Thus, according to Eq. (6), the eddy viscosity is expected to increase when z_0 increases; and both changing the surface temperature and drag appear to induce an analogous impact on the vertical diffusion. Hence, to confirm if a similar trend in the environmental flow patterns and TC tracks are observed for changing the z_0, a similar suite of cases is presented in the next section.

3.3. Environmental flow and hurricane track alterations in terms of roughness length changes

In the previous section, we assessed the impacts of surface temperature changes on environmental flow patterns. In this section, we examine if changing the roughness length induces a similar response of hurricane tracks and environmental flows to surface temperature variations. A similar set of simulations for TC tracks were conducted by changing the surface roughness length.

It has been well established that TC tracks are significantly impacted by the environmental flows (Kasahara, 1957; Miller and Moore, 1967; Roy and Kovordányi, 2012). Hence, we will determine whether the observed TC track trends are due to changes in the environmental flow patterns. To this end, in this suite of simulations, only the z_0 of low-wind

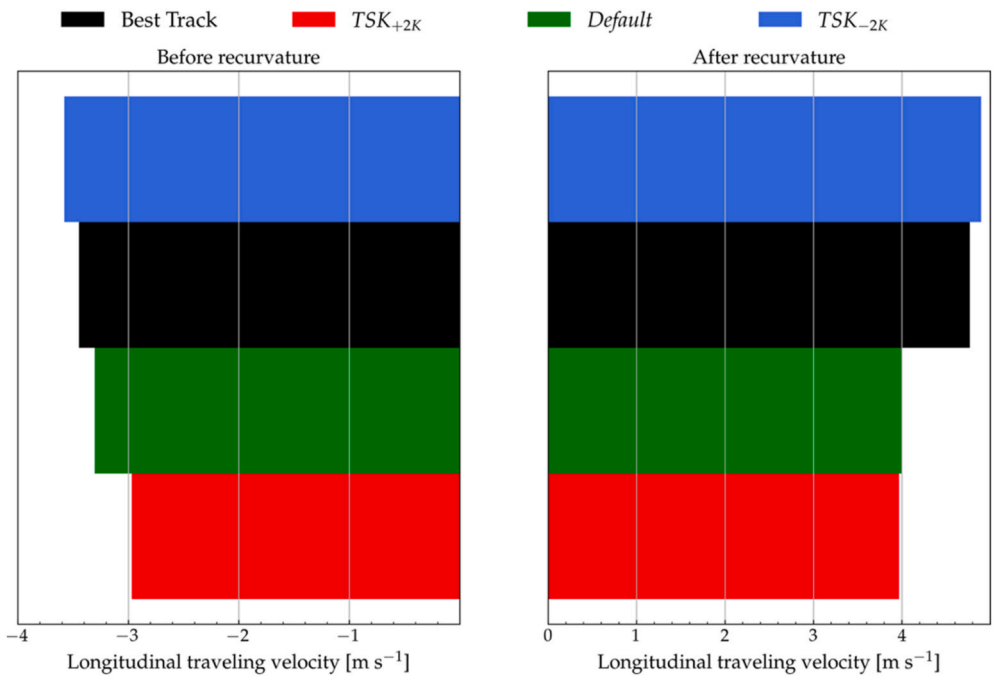

Fig. 8. Average longitudinal traveling velocity (left) before and (right) after TC's recurvature for all simulated hurricanes in terms of the surface temperature variations. The black bar depicts the average traveling velocity based on the hurricanes' best observed tracks.

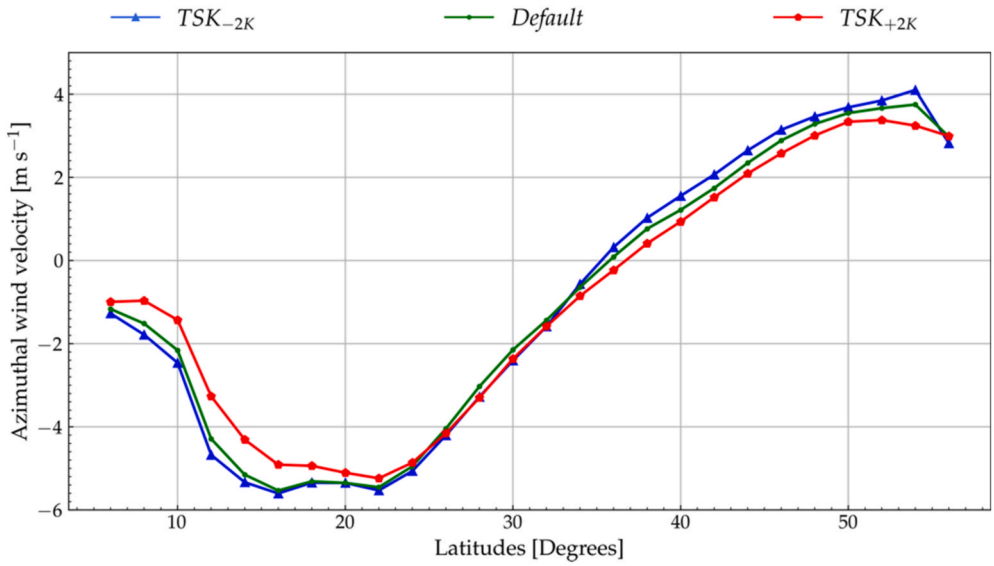

Fig. 9. Impacts of surface temperature on average azimuthal wind velocity of non-hurricane simulations. The azimuthal wind velocity is first averaged in space (over 2 degrees of latitude and entire longitudes of the domain) and then in time (over the whole simulation duration) for each case separately. Finally, the results of all non-hurricane cases are averaged and shown in this figure.

environmental flow regimes were changed to isolate the impacts of changing the surface friction to environmental flows (see Section 2.2.2). Since the z_0 of high hurricane winds is not changed in this new suite of simulations, the intensity of the simulated TCs is not considerably modulated (supplementary Fig. E1). However, for hurricane tracks a similar trend to surface temperature changes are observed (supplementary Fig. E2). When z_0 is increased, the simulated TCs move slower to the west before the recurvature and to the east after the recurvature analogous to when the surface temperature is increased.

We quantified hurricane track changes induced by altering the surface drag. The top panels of Fig. 11 show the average longitudinal translational velocities of hurricane vortex before and after recurvature. As the figure indicates, when the imposed surface z_0 increases the azimuthal translational speed of TCs decrease (red bar in Fig. 11) compared to the default cases (green bar in Fig. 11) and vice versa (blue bar in Fig. 11). This response is analogous to changing the surface temperature, which is shown in Fig. 8. Similar results were also obtained when a different surface layer parameterization (*Isftcflx* = 2) was used (see supplementary Fig. F1) indicating the generality of this finding.

To examine if the observed TC track trends are due to changes in the environmental flow patterns, we also conducted similar simulations for non-hurricane cases under surface roughness variations for the periods defined in Table 2. The bottom panel in Fig. 11 shows the results of the azimuthally averaged wind speed as a function of latitude for the

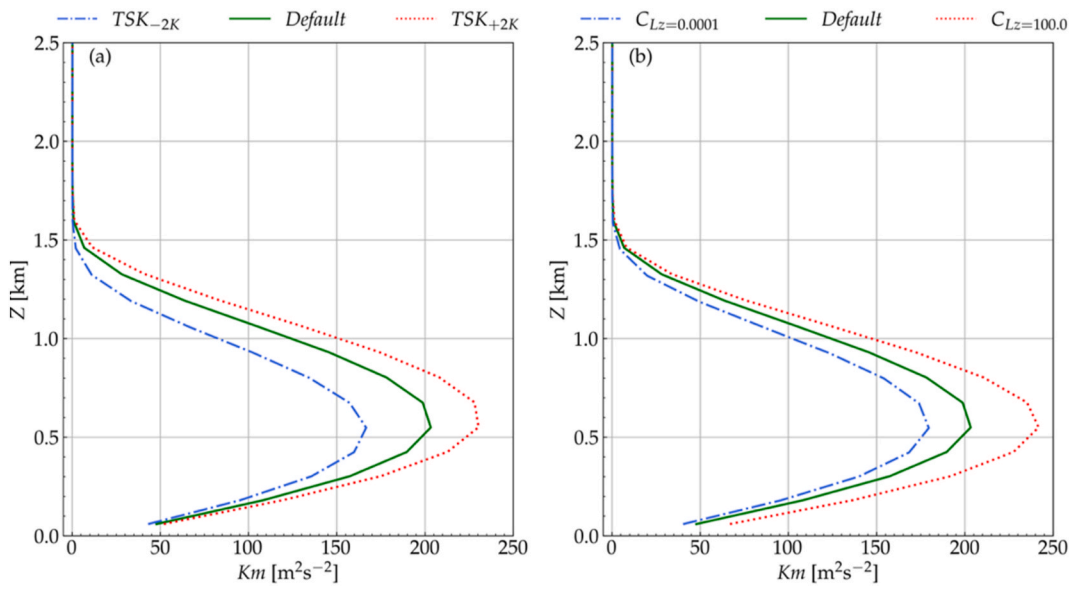

Fig. 10. Impacts of (a) surface temperature, and (b) drag changes on the vertical profiles of momentum exchange coefficient K_m. These profiles are averaged over 100 largest profiles after 30 h of simulation of case Oct_2020_32 km.

considered non-hurricane surface drag change cases. The figure indicates that by increasing the surface drag the azimuthal wind speed in environmental flows decreases (red line) and vice versa (blue line). This trend is similar and consistent with the hurricane azimuthal translational speed (compare the top and bottom panels of Fig. 11). To quantify whether altering the surface temperature or friction has a higher impact on TC track and average longitudinal velocities in our cases, we conducted a correlation analysis. Our results indicate that changing the surface roughness length had a more significant effect than varying the surface temperature on average longitudinal velocities in the considered cases (see supplementary material Fig. G.1).

To further corroborate our simulations, we compared our results with another shallow-water climate model based study which altered the surface friction damping time scale (τ_{fe}) in their simulations (Chen et al., 2007). Their results are shown as dashed lines in Fig. 11 (bottom panel). They found that a decrease of the mean drag (cyan dashed line in Fig. 11, bottom) yields an increase in the lower-layer westerlies and vice versa (orange dashed line in Fig. 11, bottom). Note that the results of Chen et al. (2007) are from a simple shallow-water global climate model and thus their domain size is much larger than our considered domain. Despite these differences in the domain and code, our results are in a qualitative agreement with their climate model simulations.

As the results indicate, increasing the surface friction tends to slow down the azimuthal wind speed in large-scale environmental flows and vice versa. Fig. 12 shows the contours of azimuthal velocity for two of the conducted non-hurricane cases. As the figure indicates, decreasing the roughness length (right panels) strengthens the surface azimuthal wind velocity (see the darker colors in the right panels) compared to the default case (middle panels) and vice versa. All these different simulations indicate that TC track trends appear to majorly root from the global environmental flow changes rather than the mesoscale hurricane vortex-environmental flow interactions. Therefore, TC tracks are considerably impacted by global and synoptic environmental flow patterns and characterizing them is vital to improve hurricane track forecasts.

4. Conclusion

This study characterizes the impacts of surface temperature and friction changes on hurricane tracks and environmental flow patterns. In total, 30 WRF hurricane simulations were conducted by varying the surface temperature and roughness length for six category 4–5 hurricanes (Earl, Gonzalo, Lorenzo, Florence, Teddy, and Maria). 60 more simulations were carried out to investigate the characteristics of environmental non-hurricane flows subject to changing surface temperature and drag, and determine their impacts on TC tracks. In summary, the key findings of this study are:

1. Increasing the surface temperature tends to intensify TCs while decreasing it generates weaker hurricanes. It was found that the average wind intensity increases by ~20 % in response to 2 K increase in the default surface temperature and vice versa. These results were consistent with other studies that projected that global warming would intensify the TCs. Note that this increase in the intensity of hurricanes can occur for just a moderate emission scenario. The hurricanes can be further intensified under a warmer climate for higher emission scenarios. To corroborate this, we conducted another set of simulations where we changed the surface temperature by 3 K (supplementary Figs. H.1 and H.2). We found that the average maximum wind intensity of hurricanes increases by ~26 % in this more extreme scenario compared to the default cases.
2. Hurricane tracks were significantly sensitive to surface temperature variations. Decreasing the surface temperature further moved the hurricane trajectories towards the west and vice versa. Note that the surface temperature variations might considerably affect the forecasting accuracy of future hurricanes that needs to be characterized in a separate retrospective analysis of climatic trends in historical TC events.
3. This trend in hurricane tracks was associated with environmental flow patterns. To show this, a set of non-hurricane cases was conducted. It was found that azimuthally averaged winds exhibit a similar trend for non-hurricane cases. Decreasing the surface temperature for such cases, increases the magnitude of azimuthally averaged winds. Increasing the surface temperature consistently decreased the magnitude of azimuthally averaged winds, which can be the case for global warming conditions under moderate and high emission scenarios. It was shown that this change in the environmental flow pattern is likely the reason behind the observed trends in hurricane tracks as a result of varying the surface temperature.
4. The surface temperature was shown to have a significant impact on surface friction and mixing in the PBL. The vertical diffusion was considerably influenced by changes in the surface temperature. It was demonstrated that vertical mixing and surface friction variations

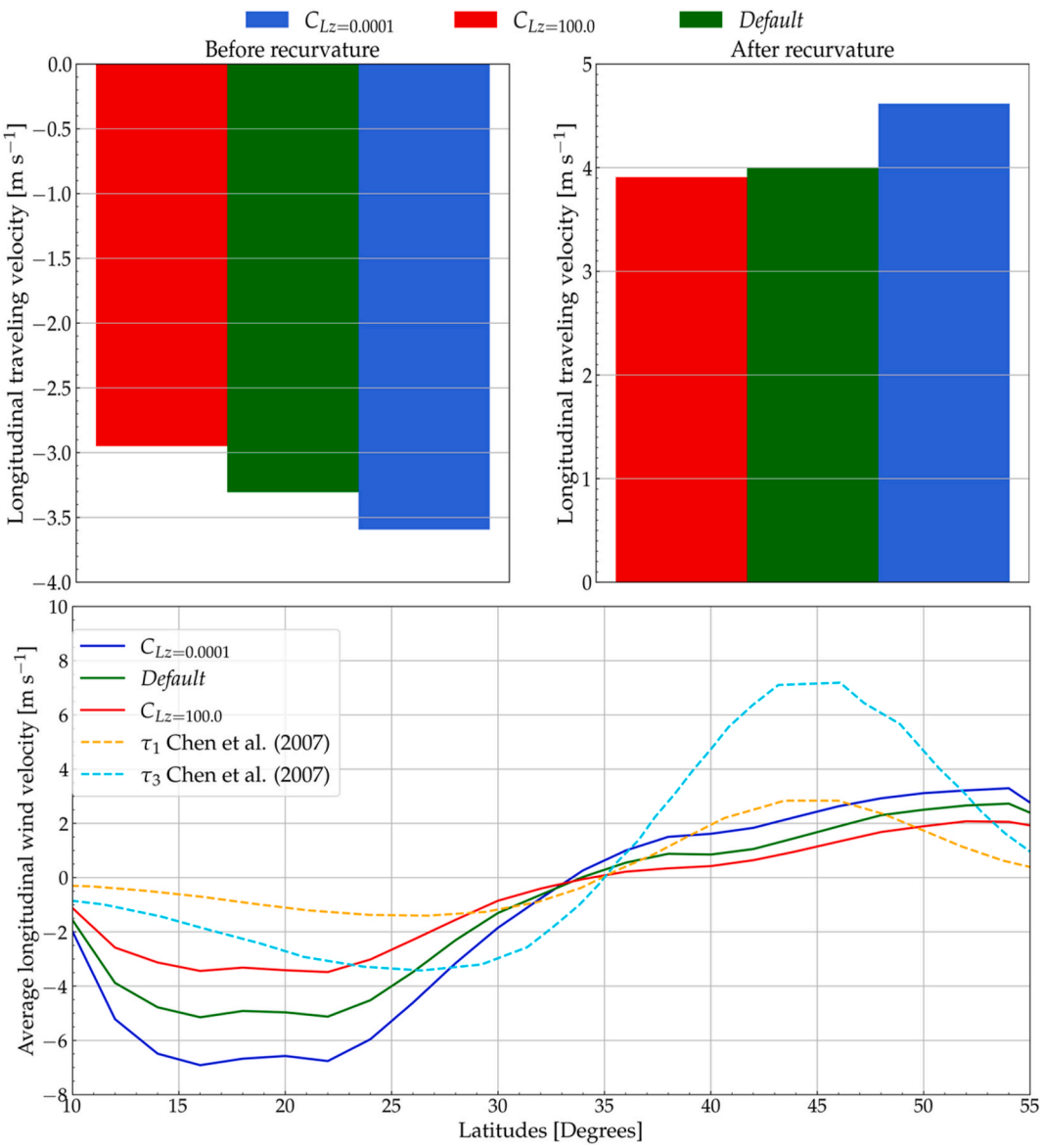

Fig. 11. Average longitudinal translational velocity before and after recurvature in terms of surface roughness changes. All hurricanes were considered for the barplots. The curves at the bottom depict the average azimuthal surface wind speed (10 m of altitude) for the non-hurricane simulations defined in Table 2.

are the cause of changes in the environmental flow patterns by conducting a similar set of simulations in which only the surface drag is altered.

5. The surface drag changes were shown to have a similar impact on hurricane tracks as surface temperature variations. Decreasing the default surface drag for low-wind regimes tends to further move the hurricanes towards the west and vice versa. Similarly, the TC track alterations were shown to be due to the changes in the environmental flow patterns. The outcomes of the non-hurricane simulations were also in agreement with a separate shallow-water climate model study verifying these results.

Our results underscore the significance of global warming on future hurricane dynamics and tracks. Increased Ocean temperature appears to significantly intensify hurricanes, and influence their tracks by decreasing their azimuthal translational speed. This was associated with the changes in the synoptic environmental flow patterns that are altered due to friction and turbulent mixing. It is thus indispensable to characterize and improve these impacts in weather/climate models to enhance TC intensity and track projections in the future.

CRediT authorship contribution statement

Oussama Romdhani: Writing – review & editing, Writing – original draft, Visualization, Validation, Software, Methodology, Investigation, Formal analysis, Data curation. **Leo Matak:** Writing – review & editing, Methodology. **Mostafa Momen:** Writing – review & editing, Writing – original draft, Supervision, Resources, Project administration, Methodology, Investigation, Funding acquisition, Formal analysis, Conceptualization.

Declaration of competing interest

The authors declare that they have no known competing financial interests or personal relationships that could have appeared to influence the work reported in this paper.

Data availability

The data for Hurricane Florence and non-hurricane simulations of August 2019 can be found in Romdhani et al. (2024). Further data will

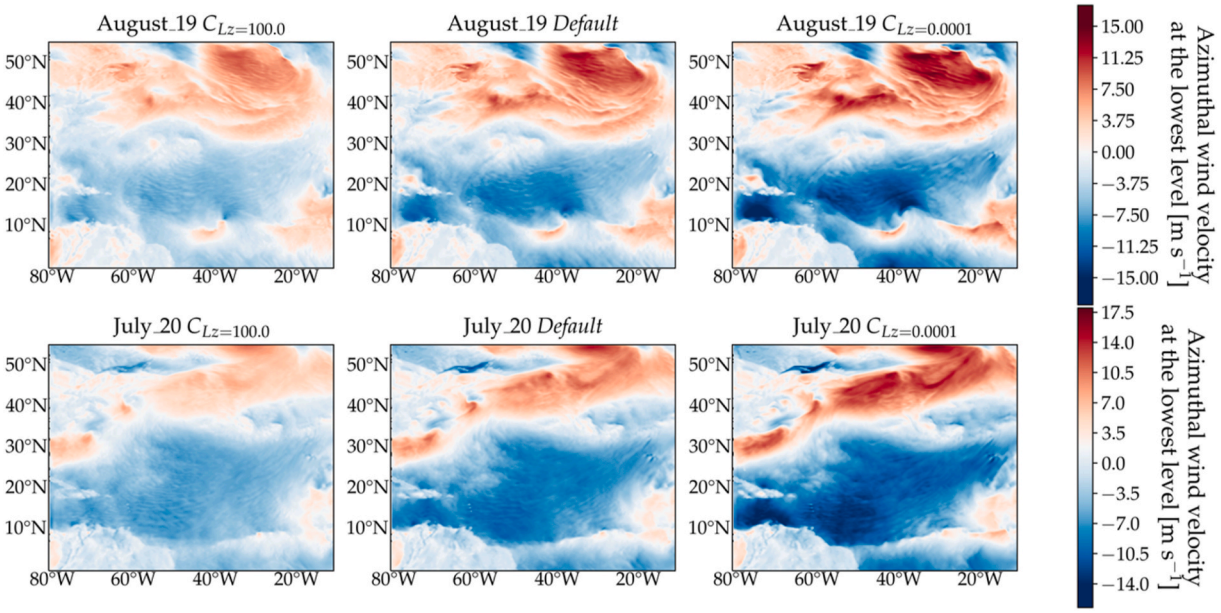

Fig. 12. Azimuthal wind velocity for two non-hurricane cases in terms of surface roughness variations. The first row corresponds to a simulation during the first week of August 2019 and the second row corresponds to a simulation during July 2020.

be made available on request.

Acknowledgments

The authors acknowledge support from the Physical and Dynamic Meteorology Program of the National Science Foundation under grant AGS-2228299 as well as the Department of Civil and Environmental Engineering at the University of Houston via startup funds. The simulations were performed on the University of Houston's computing clusters (Carya and Sabine). The authors also acknowledge computing cluster support from the National Center for Atmospheric Research (NCAR) under project number UHOU0002.

Appendix A. Supplementary data

Supplementary data to this article can be found online at https://doi.org/10.1016/j.wace.2024.100645.

References

Abarca, S.F., Corbosiero, K.L., 2011. Secondary eyewall formation in WRF simulations of hurricanes Rita and Katrina (2005). Geophys. Res. Lett. 38 https://doi.org/10.1029/2011GL047015.

Balaguru, K., Foltz, G.R., Leung, L.R., Hagos, S.M., Judi, D.R., 2018. On the Use of ocean dynamic temperature for hurricane intensity forecasting. Weather Forecast. 33, 411–418. https://doi.org/10.1175/WAF-D-17-0143.1.

Black, P.G., D'Asaro, E.A., Drennan, W.M., French, J.R., Niiler, P.P., Sanford, T.B., Terrill, E.J., Walsh, E.J., Zhang, J.A., 2007. Air–Sea exchange in hurricanes: Synthesis of observations from the Coupled boundary layer Air–Sea Transfer Experiment. Bull. Am. Meteorol. Soc. 88, 357–374. https://doi.org/10.1175/BAMS-88-3-357.

Blake, E.S., 2020. NATIONAL HURRICANE CENTER TROPICAL CYCLONE REPORT HURRICANE TEDDY (AL202020) 12-23 September 2020. Natl. Hurric. Cent.

Brown, D.P., 2015. NATIONAL HURRICANE CENTER TROPICAL CYCLONE REPORT HURRICANE Gonzalo (AL082014) 12-19 October 2014. Natl. Hurric. Cent.

Cangialosi, J.P., 2011. NATIONAL HURRICANE CENTER TROPICAL CYCLONE REPORT HURRICANE Earl (AL072010) 25 August-4 September 2010. Natl. Hurric. Cent.

Cavallo, S.M., Torn, R.D., Snyder, C., Davis, C., Wang, W., Done, J., 2013. Evaluation of the advanced hurricane WRF data Assimilation system for the 2009 Atlantic hurricane season. Mon. Weather Rev. 141, 523–541. https://doi.org/10.1175/MWR-D-12-00139.1.

Cheikh, M.I., Momen, M., 2020. The interacting effects of storm surge intensification and sea-level rise on coastal resiliency: a high-resolution turbulence resolving case study. Environ. Res. Commun. 2, 115002 https://doi.org/10.1088/2515-7620/ABC39E.

Chen, G., Held, I.M., Robinson, W.A., 2007. Sensitivity of the latitude of the surface westerlies to surface friction. J. Atmos. Sci. 64, 2899–2915. https://doi.org/10.1175/JAS3995.1.

Chen, H., Zhang, D.-L., Carton, J., Atlas, R., 2011. On the rapid intensification of Hurricane Wilma (2005). Part I: model prediction and structural changes. Wea. Forecast 26, 885–901. https://doi.org/10.1175/WAF-D-11-00001.1.

Chu, J.-E., Lee, S.-S., Timmermann, A., Wengel, C., Stuecker, M.F., Yamaguchi, R., 2023. Reduced tropical cyclone densities and ocean effects due to anthropogenic greenhouse warming. Sci. Adv. 6, eabd5109 https://doi.org/10.1126/sciadv.abd5109.

Colbert, A.J., Soden, B.J., Vecchi, G.A., Kirtman, B.P., 2013. The impact of anthropogenic climate change on North Atlantic tropical cyclone tracks. J. Clim. 26, 4088–4095. https://doi.org/10.1175/JCLI-D-12-00342.1.

Cuchiara, G.C., Li, X., Carvalho, J., Rappenglück, B., 2014. Intercomparison of planetary boundary layer parameterization and its impacts on surface ozone concentration in the WRF/Chem model for a case study in Houston/Texas. Atmos. Environ. 96, 175–185. https://doi.org/10.1016/j.atmosenv.2014.07.013.

Davis, C., Wang, W., Chen, S.S., Chen, Y., Corboseiro, K., Demaria, M., Dudhia, J., Holland, G., Klemp, J., Michalakes, J., Reeves, H., Rotunno, R., Synder, C., Xiao, Q., 2008. Prediction of landfalling hurricanes with the advanced hurricane WRF model. Mon. Weather Rev. 1990–2005. https://doi.org/10.1175/2007MWR2085.1.

Donelan, M.A., Haus, B.K., Reul, N., Plant, W.J., Stiassnie, M., Graber, H.C., Brown, O.B., Saltzman, E.S., 2004. On the limiting aerodynamic roughness of the ocean in very strong winds. Geophys. Res. Lett. 31, 1–5. https://doi.org/10.1029/2004GL019460.

Dong, K., Neumann, C.J., 1983. On the relative motion of Binary tropical cyclones. Mon. Weather Rev. 111, 945–953. https://doi.org/10.1175/1520-0493(1983)111<0945:OTRMOB>2.0.CO;2.

Emanuel, K., 2020. Evidence that hurricanes are getting stronger. Proc. Natl. Acad. Sci. U. S. A. 117, 13194–13195. https://doi.org/10.1073/PNAS.2007742117.

Emanuel, K., 2017. Will global warming Make hurricane forecasting more difficult? Bull. Am. Meteorol. Soc. 98, 495–501. https://doi.org/10.1175/BAMS-D-16-0134.1.

Emanuel, K., 2005. Increasing destructiveness of tropical cyclones over the past 30 years. Nature 436, 686–688. https://doi.org/10.1038/nature03906.

Emanuel, K.A., 1997. Some Aspects of hurricane Inner-Core dynamics and Energetics. J. Atmos. Sci. 54, 1014–1026. https://doi.org/10.1175/1520-0469(1997)054<1014:SAOHIC>2.0.CO;2.

Fierro, A.O., Rogers, R.F., Marks, F.D., Nolan, D.S., 2009. The impact of Horizontal grid spacing on the Microphysical and Kinematic structures of strong tropical cyclones simulated with the WRF-ARW model. Mon. Weather Rev. 137, 3717–3743. https://doi.org/10.1175/2009MWR2946.1.

Franklin, J.L., 1990. Dropwindsonde observations of the environmental flow of hurricane Josephine (1984): relationships to vortex motion. Mon. Weather Rev. 118, 2732–2744. https://doi.org/10.1175/1520-0493(1990)118<2732:DOOTEF>2.0.CO;2.

Fyfe, J.C., Boer, G.J., Flato, G.M., 1999. The Arctic and Antarctic oscillations and their projected changes under global warming. Geophys. Res. Lett. 26, 1601–1604. https://doi.org/10.1029/1999GL900317.

Galarneau, T.J., Davis, C.A., 2013. Diagnosing forecast Errors in tropical cyclone motion. Mon. Weather Rev. 141, 405–430. https://doi.org/10.1175/MWR-D-12-00071.1.

Garner, A.J., Kopp, R.E., Horton, B.P., 2021. Evolving tropical cyclone tracks in the North Atlantic in a warming climate. Earth's Futur 9, e2021EF002326. https://doi.org/10.1029/2021EF002326.

Garratt, J.R., 1994. Review: the atmospheric boundary layer. Earth Sci. Rev. 37, 89–134. https://doi.org/10.1016/0012-8252(94)90026-4.
Gopalakrishnan, S.G., Marks, F., Zhang, J.A., Zhang, X., Bao, J.-W., Tallapragada, V., 2013. A study of the impacts of vertical diffusion on the Structure and intensity of the tropical cyclones using the high-resolution HWRF system. J. Atmos. Sci. 70, 524–541. https://doi.org/10.1175/JAS-D-11-0340.1.
Haigh, J.D., Blackburn, M., Day, R., 2005. The Response of Tropospheric Circulation to Perturbations in Lower-Stratospheric Temperature.
Hall, T.M., Kossin, J.P., Thompson, T., McMahon, J., 2021. U.S. Tropical cyclone Activity in the 2030s based on projected changes in tropical sea surface temperature. J. Clim. 34, 1321–1335. https://doi.org/10.1175/JCLI-D-20-0342.1.
Hong, S.-Y., 2010. A new stable boundary-layer mixing scheme and its impact on the simulated East Asian summer monsoon. Q. J. R. Meteorol. Soc. 136, 1481–1496. https://doi.org/10.1002/qj.665.
Hong, S.-Y., Noh, Y., Dudhia, J., 2006. A new vertical diffusion package with an Explicit Treatment of Entrainment processes. Mon. Weather Rev. 134, 2318–2341. https://doi.org/10.1175/MWR3199.1.
Hosannah, N., Ramamurthy, P., Marti, J., Munoz, J., González, J.E., 2021. Impacts of hurricane Maria on Land and convection modification over Puerto Rico. J. Geophys. Res. Atmos. 126, e2020JD032493 https://doi.org/10.1029/2020JD032493.
Intergovernmental Panel on Climate Change, 2013. Climate Change 2013 – the Physical Science Basis: Working Group I Contribution to the Fifth Assessment Report of the Intergovernmental Panel on Climate Change. Cambridge University Press, Cambridge. https://doi.org/10.1017/CBO9781107415324.
Intergovernmental Panel on Climate Change (IPCC), 2023. Weather and climate extreme events in a changing climate. In: Climate Change 2021 – the Physical Science Basis: Working Group I Contribution to the Sixth Assessment Report of the Intergovernmental Panel on Climate Change. Cambridge University Press, Cambridge, pp. 1513–1766. https://doi.org/10.1017/9781009157896.013.
Jarosz, E., Mitchell, D.A., Wang, D.W., Teague, W.J., 2007. Bottom-up Determination of air-sea momentum exchange under a major tropical cyclone. Science (80- 315, 1707–1709. https://doi.org/10.1126/science.1136466.
Jiménez, P.A., Dudhia, J., González-Rouco, J.F., Navarro, J., Montávez, J.P., García-Bustamante, E., 2012. A Revised scheme for the WRF surface layer formulation. Mon. Weather Rev. 140, 898–918. https://doi.org/10.1175/MWR-D-11-00056.1.
Kasahara, A., 1957. The numerical prediction of hurricane movement with the barotropic model. J. Atmos. Sci. 14, 386–402.
Kepert, J.D., 2012. Choosing a boundary layer parameterization for tropical cyclone modeling. Mon. Weather Rev. 140, 1427–1445. https://doi.org/10.1175/MWR-D-11-00217.1.
Kidston, J., Vallis, G.K., Dean, S.M., Renwick, J.A., 2011. Can the increase in the eddy length scale under global warming cause the poleward shift of the jet streams? J. Clim. 24, 3764–3780. https://doi.org/10.1175/2010JCLI3738.1.
Knutson, T., Camargo, S.J., Chan, J.C.L., Emanuel, K., Ho, C.-H., Kossin, J., Mohapatra, M., Satoh, M., Sugi, M., Walsh, K., Wu, L., 2020. Tropical cyclones and climate change assessment: Part II: projected response to anthropogenic warming. Bull. Am. Meteorol. Soc. 101, E303–E322. https://doi.org/10.1175/BAMS-D-18-0194.1.
Knutson, T., Camargo, S.J., Chan, J.C.L., Emanuel, K., Ho, C.-H., Kossin, J., Mohapatra, M., Satoh, M., Sugi, M., Walsh, K., Wu, L., 2019. Tropical cyclones and climate change assessment: Part I: Detection and Attribution. Bull. Am. Meteorol. Soc. 100, 1987–2007. https://doi.org/10.1175/BAMS-D-18-0189.1.
Knutson, T.R., McBride, J.L., Chan, J., Emanuel, K., Holland, G., Landsea, C., Held, I., Kossin, J.P., Srivastava, A.K., Sugi, M., 2010. Tropical cyclones and climate change. Nat. Geosci. 3, 157–163. https://doi.org/10.1038/ngeo779.
Kossin, J.P., 2018. A global slowdown of tropical-cyclone translation speed. Nature 558, 104–107. https://doi.org/10.1038/s41586-018-0158-3.
Kossin, J.P., Camargo, S.J., 2009. Hurricane track variability and secular potential intensity trends. Clim. Change 97, 329–337. https://doi.org/10.1007/s10584-009-9748-2.
Kossin, J.P., Camargo, S.J., Sitkowski, M., 2010. Climate modulation of North Atlantic hurricane tracks. J. Clim. 23, 3057–3076. https://doi.org/10.1175/2010JCLI3497.1.
Kushner, P.J., Held, I.M., Delworth, T.L., 2001. Southern hemisphere atmospheric circulation response to global warming. J. Clim. 14, 2238–2249. https://doi.org/10.1175/1520-0442(2001)014<0001:SHACRT>2.0.CO;2.
Li, D., Bou-Zeid, E., Oppenheimer, M., 2014. The effectiveness of cool and green roofs as urban heat island mitigation strategies. Environ. Res. Lett. 9, 55002 https://doi.org/10.1088/1748-9326/9/5/055002.
Li, M., Zhang, J.A., Matak, L., Momen, M., 2023. The impacts of adjusting momentum roughness length on strong and weak hurricanes forecasts: a comprehensive analysis of weather simulations and observations. Mon. Weather Rev. https://doi.org/10.1175/MWR-D-22-0191.1.
Marsooli, R., Lin, N., Emanuel, K., Feng, K., 2019. Climate change exacerbates hurricane flood hazards along US Atlantic and Gulf Coasts in spatially varying patterns. Nat. Commun. 10, 1–9. https://doi.org/10.1038/s41467-019-11755-z.
Matak, L., Momen, M., 2023. The role of vertical diffusion parameterizations in the dynamics and accuracy of simulated intensifying hurricanes. Boundary-Layer Meteorol. 188, 389–418. https://doi.org/10.1007/s10546-023-00818-w.
Mei, W., Xie, S.-P., 2016. Intensification of landfalling typhoons over the northwest Pacific since the late 1970s. Nat. Geosci. 9, 753–757. https://doi.org/10.1038/ngeo2792.
Meinshausen, M., Nicholls, Z.R.J., Lewis, J., Gidden, M.J., Vogel, E., Freund, M., Beyerle, U., Gessner, C., Nauels, A., Bauer, N., Canadell, J.G., Daniel, J.S., John, A., Krummel, P.B., Luderer, G., Meinshausen, N., Montzka, S.A., Rayner, P.J., Reimann, S., Smith, S.J., van den Berg, M., Velders, G.J.M., Vollmer, M.K., Wang, R. H.J., 2020. The shared socio-economic pathway (SSP) greenhouse gas concentrations and their extensions to 2500. Geosci. Model Dev. (GMD) 13, 3571–3605. https://doi.org/10.5194/gmd-13-3571-2020.
Meinshausen, M., Smith, S.J., Calvin, K., Daniel, J.S., Kainuma, M.L.T., Lamarque, J.-F., Matsumoto, K., Montzka, S.A., Raper, S.C.B., Riahi, K., Thomson, A., Velders, G.J.M., van Vuuren, D.P.P., 2011. The RCP greenhouse gas concentrations and their extensions from 1765 to 2300. Clim. Change 109, 213. https://doi.org/10.1007/s10584-011-0156-z.
Miller, B.I., Moore, P.L., 1967. American meteorological Society-Elections. Bull. Am. Meteorol. Soc. 41, 59–63. https://doi.org/10.1080/00431672.1967.9932750.
Miller, R.L., Schmidt, G.A., Shindell, D.T., 2006. Forced Annular Variations in the 20th Century Intergovernmental Panel on Climate Change Fourth Assessment Report Models.
Ming, J., Zhang, J.A., Li, X., Pu, Z., Momen, M., 2023. Observational estimates of turbulence parameters in the atmospheric surface layer of landfalling tropical cyclones. J. Geophys. Res. Atmos. 128, e2022JD037768 https://doi.org/10.1029/2022JD037768.
Momen, M., 2022. Baroclinicity in stable atmospheric boundary layers: characterizing turbulence structures and collapsing wind profiles via reduced models and large-eddy simulations. Q. J. R. Meteorol. Soc. 148, 76–96. https://doi.org/10.1002/qj.4193.
Momen, M., Bou-Zeid, E., 2017. Mean and turbulence dynamics in unsteady Ekman boundary layers. J. Fluid Mech. 816, 209–242. https://doi.org/10.1017/jfm.2017.76.
Momen, M., Bou-Zeid, E., 2016. Large-eddy simulations and Damped-Oscillator models of the unsteady Ekman boundary layer. J. Atmos. Sci. 73, 25–40. https://doi.org/10.1175/JAS-D-15-0038.1.
Momen, M., Bou-Zeid, E., Parlange, M.B., Giometto, M., 2018. Modulation of mean wind and turbulence in the atmospheric boundary layer by Baroclinicity. J. Atmos. Sci. 75, 3797–3821. https://doi.org/10.1175/JAS-D-18-0159.1.
Momen, M., Parlange, M.B., Giometto, M.G., 2021. Scrambling and Reorientation of Classical atmospheric boundary layer turbulence in hurricane winds. Geophys. Res. Lett. 48, e2020GL091695 https://doi.org/10.1029/2020GL091695.
Nasrollahi, N., AghaKouchak, A., Li, J., Gao, X., Hsu, K., Sorooshian, S., 2012. Assessing the impacts of different WRF Precipitation physics in hurricane simulations. Weather Forecast. 27, 1003–1016. https://doi.org/10.1175/WAF-D-10-05000.1.
NCAR, 2019. User's Guides for the Advanced Research WRF (ARW) Modeling System, Version 4 456.
Nolan, D.S., Stern, D.P., Zhang, J.A., 2009. Evaluation of planetary boundary layer parameterizations in tropical cyclones by comparison of in Situ observations and high-resolution simulations of hurricane Isabel (2003). Part II: Inner-Core boundary layer and eyewall Structure. Mon. Weather Rev. 137, 3675–3698. https://doi.org/10.1175/2009MWR2786.1.
Olivo, Y., Hamidi, A., Ramamurthy, P., 2017. Spatiotemporal variability in building energy use in New York City. Energy 141, 1393–1401. https://doi.org/10.1016/j.energy.2017.11.066.
Pasch, R.J., Penny, A.B., Berg, R., 2023. NATIONAL HURRICANE CENTER TROPICAL CYCLONE REPORT HURRICANE MARIA (AL152017) 16-30 September 2017. Natl. Hurric. Cent.
Polvani, L.M., Kushner, P.J., 2002. Tropospheric Response to Stratospheric Perturbations in a Relatively Simple General Circulation Model.
Powell, M.D., Vickery, P.J., Reinhold, T.A., 2003. Reduced drag coefficient for high wind speeds in tropical cyclones. Nature 422, 279–283. https://doi.org/10.1038/nature01481.
Powers, J.G., Klemp, J.B., Skamarock, W.C., Davis, C.A., Dudhia, J., Gill, D.O., Coen, J.L., Gochis, D.J., Ahmadov, R., Peckham, S.E., Grell, G.A., Michalakes, J., Trahan, S., Benjamin, S.G., Alexander, C.R., Dimego, G.J., Wang, W., Schwartz, C.S., Romine, G. S., Liu, Z., Snyder, C., Chen, F., Barlage, M.J., Yu, W., Duda, M.G., 2017. The weather research and forecasting model: overview, system Efforts, and future directions. Bull. Am. Meteorol. Soc. 98, 1717–1737. https://doi.org/10.1175/BAMS-D-15-00308.1.
Robinson, W.A., 1997. Dissipation Dependence of the Jet Latitude.
Rogelj, J., Popp, A., Calvin, K.V., Luderer, G., Emmerling, J., Gernaat, D., Fujimori, S., Strefler, J., Hasegawa, T., Marangoni, G., Krey, V., Kriegler, E., Riahi, K., van Vuuren, D.P., Doelman, J., Drouet, L., Edmonds, J., Fricko, O., Harmsen, M., Havlík, P., Humpenöder, F., Stehfest, E., Tavoni, M., 2018. Scenarios towards limiting global mean temperature increase below 1.5 °C. Nat. Clim. Chang. 8, 325–332. https://doi.org/10.1038/s41558-018-0091-3.
Romdhani, O., Matak, L., Momen, M., 2024. Hurricane track trends and environmental flow patterns under surface temperature changes and roughness length variations. https://doi.org/10.7910/DVN/E8SCDQ. Harvard Dataverse, V1.
Romdhani, O., Zhang, J.A., Momen, M., 2022. Characterizing the impacts of turbulence Closures on real hurricane forecasts: a comprehensive Joint assessment of grid resolution, Horizontal turbulence models, and Horizontal mixing length. J. Adv. Model. Earth Syst. 14, e2021MS002796 https://doi.org/10.1029/2021MS002796.
Roy, C., Kovordányi, R., 2012. Tropical cyclone track forecasting techniques - a review. Atmos. Res. 104– 105, 40–69. https://doi.org/10.1016/j.atmosres.2011.09.012.
Sabet, F., Yi, Y., Thomas, L., Momen, M., 2022. Characterizing Mean and Turbulent Structures of Hurricane Winds via Large-Eddy Simulations. Center for Turbulence Research Proceedings of the Summer Program, pp. 311–321.
Schleussner, C.-F., Rogelj, J., Schaeffer, M., Lissner, T., Licker, R., Fischer, E.M., Knutti, R., Levermann, A., Frieler, K., Hare, W., 2016. Science and policy characteristics of the Paris Agreement temperature goal. Nat. Clim. Chang. 6, 827–835. https://doi.org/10.1038/nclimate3096.
Shaw, T.A., Baldwin, M., Barnes, E.A., Caballero, R., Garfinkel, C.I., Hwang, Y.-T., Li, C., O'Gorman, P.A., Rivière, G., Simpson, I.R., Voigt, A., 2016. Storm track processes

and the opposing influences of climate change. Nat. Geosci. 9, 656–664. https://doi.org/10.1038/ngeo2783.
Skamarock, W.C., Klemp, J.B., Dudhia, J., Gill, D.O., Zhiquan, L., Berner, J., Wang, W., Powers, J.G., Duda, M.G., Barker, D.M., Huang, X.-Y., 2019. A Description of the Advanced Research WRF Model Version 4, NCAR Technical Note NCAR/TN-475+STR.
Soloviev, A.V., Lukas, R., Donelan, M.A., Haus, B.K., Ginis, I., 2014. The air-sea interface and surface stress under tropical cyclones. Sci. Rep. 4, 1–6. https://doi.org/10.1038/srep05306.
Son, S.W., Lee, S., 2005. The Response of Westerly Jets to Thermal Driving in a Primitive Equation Model.
Stewart, S.R., Berg, R., 2019. NATIONAL HURRICANE CENTER TROPICAL CYCLONE REPORT HURRICANE FLORENCE (AL062018) 31 August-17 September 2018. Natl. Hurric. Cent.
Studholme, J., Fedorov, A.V., Gulev, S.K., Emanuel, K., Hodges, K., 2022. Poleward expansion of tropical cyclone latitudes in warming climates. Nat. Geosci. 15, 14–28. https://doi.org/10.1038/s41561-021-00859-1.
Thompson, D.W.J., Solomon, S., 2002. Interpretation of recent southern hemisphere climate change. Science 296, 895–899. https://doi.org/10.1126/SCIENCE.1069270.
Vaughan, M.T., Fovell, R.G., 2021. The influence of boundary layer mixing Strength on the Evolution of a Baroclinic cyclone. Mon. Weather Rev. 149, 661–678. https://doi.org/10.1175/MWR-D-20-0264.1.
Velden, C.S., Leslie, L.M., 1991. The basic relationship between tropical cyclone intensity and the Depth of the environmental steering layer in the Australian region. Weather Forecast. 6, 244–253. https://doi.org/10.1175/1520-0434(1991)006<0244:TBRBTC>2.0.CO;2.
Walsh, K.J.E., Camargo, S.J., Knutson, T.R., Kossin, J., Lee, T.-C., Murakami, H., Patricola, C., 2019. Tropical cyclones and climate change. Trop. Cyclone Res. Rev. 8, 240–250. https://doi.org/10.1016/j.tcrr.2020.01.004.
Wang, B., Elsberry, R.L., Yuqing, W., Liguang, W., 1998. Dynamics in tropical cyclone motion: a review. Chinese J. Atmos. Sci. 22, 416–434.
Wu, Y., Ting, M., Seager, R., Huang, H.-P., Cane, M.A., 2011. Changes in storm tracks and energy transports in a warmer climate simulated by the GFDL CM2.1 model. Clim. Dyn. 37, 53–72. https://doi.org/10.1007/s00382-010-0776-4.
Yang, J., Wang, Z.-H., Chen, F., Miao, S., Tewari, M., Voogt, J.A., Myint, S., 2015. Enhancing Hydrologic Modelling in the Coupled weather research and forecasting–urban Modelling system. Boundary-Layer Meteorol. 155, 87–109. https://doi.org/10.1007/s10546-014-9991-6.
Yu, B., Gan Chowdhury, A., Masters, F.J., 2008. Hurricane wind Power Spectra, Cospectra, and Integral length scales. Boundary-Layer Meteorol. 129, 411–430. https://doi.org/10.1007/s10546-008-9316-8.
Zelinsky, D.A., 2019. NATIONAL HURRICANE CENTER TROPICAL CYCLONE REPORT HURRICANE LORENZO (AL132019) 23 September-2 October 2019. Natl. Hurric. Cent.
Zhang, C., Wang, Y., Hamilton, K., 2011. Improved Representation of boundary layer Clouds over the Southeast Pacific in ARW-WRF using a modified Tiedtke Cumulus parameterization scheme. Mon. Weather Rev. 139, 3489–3513. https://doi.org/10.1175/MWR-D-10-05091.1.
Zhang, J.A., Drennan, W.M., Black, P.G., French, J.R., 2009. Turbulence Structure of the hurricane boundary layer between the outer Rainbands. J. Atmos. Sci. 66, 2455–2467. https://doi.org/10.1175/2009JAS2954.1.
Zhang, J.A., Nolan, D.S., Rogers, R.F., Tallapragada, V., 2015. Evaluating the impact of Improvements in the boundary layer parameterization on hurricane intensity and Structure forecasts in HWRF. Mon. Weather Rev. 143, 3136–3155. https://doi.org/10.1175/MWR-D-14-00339.1.